Bi-hormonal Linear Time-Varying Model Predictive Control for Blood Glucose Regulation in Type 1 Diabetes Patients

Kalisvaart, Dylan; Bonekamp, Jorge; Grammatico, Sergio

DOI
10.1109/CCTA54093.2023.10252997

Publication date
2023

Document Version
Final published version

Published in
Proceedings of the 2023 IEEE Conference on Control Technology and Applications, CCTA 2023

2023 IEEE Conference on Control Technology and Applications (CCTA)
August 16-18, 2023. Bridgetown, Barbados

Bi-hormonal Linear Time-Varying Model Predictive Control for Blood Glucose Regulation in Type 1 Diabetes Patients

Dylan Kalisvaart, Jorge Bonekamp and Sergio Grammatico

2023 IEEE Conference on Control Technology and Applications (CCTA) | 979-8-3503-3544-6/23/$31.00 ©2023 IEEE | DOI: 10.1109/CCTA54093.2023.10252997

***Abstract*—We study predictive control for blood glucose regulation in patients with type 1 diabetes mellitus. We determine optimal control actions for insulin and glucagon infusion via linear time-varying model predictive control (LTV MPC) and dynamic linerization around the state trajectory predicted. Through *in silico* implementation of a comprehensive nonlinear model, we show that our proposed controller is able to reject meal disturbances, retain normoglycemia afterwards and significantly outperform standard linearized MPC.**

I. Introduction

It was estimated that in 2019 around 463 million people worldwide suffered from diabetes, from which approximately 10% consisted of type 1 diabetes mellitus (T1DM) [1]. Patients with T1DM suffer from a deficiency of insulin secretion by the pancreas, which causes elevated blood glucose (BG) levels. Untreated, T1DM results in sustained hyperglycemia (BG $>$ 7.8 mmol L^{-1}), which will result in severe short-term and long-term complications [2]. T1DM patients depend on external insulin infusion, which typically consists of a basal insulin infusion and an extra insulin bolus before meal intake, guided by manual glucose measurements. Infusion of too much insulin can result in dangerously low glucose levels, or hypoglycemia (BG $<$ 3.9 mmol L^{-1}), which in turn can lead to a number of complications and even coma [3]–[5].

Unfortunately, the usual procedure of measuring glucose levels and manual insulin infusion is inconvenient for patients suffering from T1DM and it generally does not ensure good regulation of BG concentration. This has motivated extensive research on glycemic control strategies, such as the so-called artificial pancreas. The initial research in the 1970s in [6] and [7] supported the development of the first glucose controlled insulin infusion systems. Thereafter, more advanced control algorithms for the artificial pancreas have been developed, for example expert PID-type controllers [8]–[10] that require some form of gain scheduling to simultaneously deal with both BG regulation and meal disturbance rejection.

The design of an effective controller is further complicated by the time-delays present in subcutaneous glucose measurements and hormone absorption. On the other hand, the glucose intake through meals follows a predictable pattern. An oral glucose absorption model was proposed in [11] and [12], where the authors concluded that incorporating such a model in the controllers benefits BG regulation. Consequently, Model Predictive Control (MPC) has been recognized as a good candidate for glucose regulation [13]. In short, MPC is a control approach that uses a process model to predict the future system evolution (state trajectory) and iteratively calculates the optimal control action by minimizing a cost function. Early studies on the use of MPC in glucoregulatory control showed promising results and performance [14], [15]. In [16], an *in silico* trial has shown that even linearized MPC (namely, MPC devised from a linear model) achieves significantly better glucose regulation compared to PID control. The use of (advanced) MPC strategies has become even more prevalent in recent studies [17], [18]. Among others, a nonlinear MPC strategy was proposed in [12] where it was shown that, with a sufficiently accurate model, MPC has the potential to provide extremely good BG regulation. However, from a technical perspective, nonlinear models generate non-convex optimization problems within MPC, thus convergence to a global optimum cannot be guaranteed. In [19], the authors proposed a bi-hormonal MPC controller that administers both insulin and glucagon. In particular, it was shown that hypoglycemia is more easily avoided for aggressive insulin delivery if glucagon is used as an additional input. In fact, glucagon is a hormone that has the effect of increasing glucose concentrations. Indeed, it was shown in [20] that glucagon helps to recover from hypoglycemia faster. However, glucagon infusion should be handled carefully, because large glucagon doses may have adverse effects (e.g. nausea) [20].

In this paper, we use a *time-varying linearization* of a bi-hormonal physiological model within MPC. Specifically, we propose a bi-hormonal version of the Hovorka model [12], augmented with a glucagon subsystem similar to that in [19]. Via representative numerical simulations, we show that our proposed approach, a linear-time-varying MPC (LTV-MPC), significantly outperforms the standard (linear-time-invariant) MPC approach in terms of glucoregulatory performance. Moreover, our numerical results show that the use of glucagon as a control input in our LTV-MPC generates a more effective meal disturbance rejection while avoiding hypoglycemia.

II. Mathematical Model

In [12] and [21], a nonlinear model of glucose kinetics, regulated only by insulin, is proposed - see Subsections II-A and II-B. In [19], the Bergman minimal model [22] is extended to account for the effect of glucagon on glucose production.

The authors are with the Delft Center for Systems and Control (DCSC), TU Delft, The Netherlands. E-mail addresses: {d.kalisvaart, s.grammatico}@tudelft.nl, jorgebonekamp@gmail.com.

A. Glucose subsystem

A complete model of the the glucose-insulin dynamics consists of eight first-order ordinary differential equations [12]. The dynamics of the measurable and non-measurable glucose mass states, $Q_1(t)$ and $Q_2(t)$ (mmol kg^{-1}), read as follows:

$$\dot{Q}_1(t) = -F_{01}^c(G(t)) - x_1(t)Q_1(t) + k_{12}Q_2(t) - F_R(G(t)) + \text{EGP}_0(1 - x_3(t)) + c_{\text{conv}}U_G(t) + Y(t)Q_1(t) \quad (1)$$

$$\dot{Q}_2(t) = x_1(t)Q_1(t) - (k_{12} + x_2(t))Q_2(t). \quad (2)$$

k_{12} is the transfer rate between the non-measurable and measurable compartments. EGP_0 is the endogenous glucose production (assumed constant). F_{01}^c is the insulin-independent glucose flux and F_R is the renal glucose clearance:

$$F_{01}^c(G(t)) = \begin{cases} F_{01} & \text{if } G(t) \geq 4.5 \text{ mmol } L^{-1} \\ F_{01}G(t)/4.5 & \text{otherwise} \end{cases} \quad (3)$$

$$F_R(G(t)) = \begin{cases} 0.003(G(t) - 9)V_G & \text{if } G(t) \geq 9 \text{ mmol } L^{-1} \\ 0 & \text{otherwise.} \end{cases} \quad (4)$$

Thus, $F_{01}^c(G(t))$ and $F_R(G(t))$ are piecewise linear terms that change value whenever a hyperglycemia or hypoglycemia occur. These values depend on the BG concentration, $G(t)$ (mmol L^{-1}), which is directly related to the measurable glucose mass through the glucose distribution volume, V_G:

$$G(t) = Q_1(t)/V_G. \quad (5)$$

The effect of insulin on the glucose mass states $x_1(t)$, $x_2(t)$ and $x_3(t)$ is discussed in Subsection II-B. The effect of glucagon on the glucose mass states is modeled through $Y(t)$. In Subsection II-C, we describe how glucagon dynamics using exogenous glucagon input can be modeled through the term $Y(t)$. Next, U_G (g min^{-1}) models the gut absorption rate. Unless specified otherwise, we treat U_G as a known exogenous disturbance. In [12], an expression for U_G is derived as

$$U_G(t) = \frac{D_G A_G}{t_{\max,G}^2} \cdot t \cdot \exp\left(-t/t_{\max,G}\right). \quad (6)$$

The constants D_G, A_G and $t_{\max,G}$ are the amount of carbohydrates digested, carbohydrate bio-availability and time-to-maximum carbohydrate absorption, respectively. Note that in (1), U_G is multiplied by a unit conversion factor c_{conv}, not explicitly mentioned in [12], in order to directly add it in the glucose mass concentration dynamics. Specifically, $c_{\text{conv}} = \frac{M_g}{\text{BW}} \cdot 10^3$, where M_g (g mol^{-1}) is the molar mass of glucose and BW (kg) is the patients body-weight.

B. Insulin subsystem

The insulin effect on glucose production is modeled by three different insulin action states that appear in (1) and (2). The states $x_1(t)$ and $x_2(t)$ in (min^{-1}) represent the insulin effect on glucose distribution and disposal, respectively. The endogenous glucose production is inhibited by $x_3(t)$. Thus:

$$\dot{x}_1(t) = -k_{a1}x_1(t) + k_{b1}I(t) \quad (7)$$

$$\dot{x}_2(t) = -k_{a2}x_2(t) + k_{b2}I(t) \quad (8)$$

$$\dot{x}_3(t) = -k_{a3}x_3(t) + k_{b3}I(t). \quad (9)$$

k_a and k_b are the deactivation and activation rate constants of the insulin action states. The activation rate depends on the plasma insulin concentration, $I(t)$. The plasma insulin concentration can be controlled by administering insulin. However, the insulin absorption is delayed by a two-compartment chain model. For the insulin concentration dynamics (mU kg^{-1}) of the compartments $S_1(t)$ and $S_2(t)$ we have:

$$\dot{S}_1(t) = u_I(t) - \frac{S_1(t)}{t_{\max,I}}, \ \dot{S}_2(t) = \frac{S_1(t)}{t_{\max,I}} - \frac{S_2(t)}{t_{\max,I}}. \quad (10)$$

Here, $u_I(t)$ (mU kg^{-1} min^{-1}) is the insulin administered in the first compartment through bolus and infusion. The concentration exponentially decays with time-constant $t_{\max,I}$, which is the time-to-maximum insulin absorption constant. The plasma insulin dynamics can then be modeled as

$$\dot{I}(t) = \frac{S_2(t)}{V_I t_{\max,I}} - k_{\text{e}}I(t) \quad (11)$$

where $I(t)$ is the plasma insulin concentration (mU L^{-1}), V_I is the insulin distribution volume and k_{e} is the fractional elimination rate constant.

C. Glucagon subsystem

We include glucagon as an exogenous input. The effect of glucagon on the glucose mass can be described through a stand-alone subsystem, consisting of four linear ordinary differential equations [19]. Thus, we extend the glucose-insulin model of subsections II-A and II-B via a similar stand-alone subsystem. Similarly to that of insulin, it consists of a two-compartment absorption chain, described by the states $Z_1(t)$ and $Z_2(t)$ (ng kg^{-1}). Infusing glucagon leads, via the two-compartment chain, to an elevated glucagon concentration state, $N(t)$ (pg mL^{-1}). In turn, this state has an effect on the glucose concentration through the glucagon action state, $Y(t)$ (min^{-1}). In the following, Equations (12)-(13) describe the glucagon absorption model and Equation (14) represents the glucagon action on the glucose production:

$$\dot{Z}_1(t) = u_N(t) - \frac{Z_1(t)}{t_{\max,N}}, \ \dot{Z}_2(t) = \frac{Z_1(t)}{t_{\max,N}} - \frac{Z_2(t)}{t_{\max,N}} \quad (12)$$

$$\dot{N}(t) = -k_N(N(t) - N_b) + \frac{Z_2(t)}{V_N t_{\max,N}} \quad (13)$$

$$\dot{Y}(t) = -pY(t) + pS_N(N(t) - N_b). \quad (14)$$

$u_N(t)$ is the glucagon input (ng kg^{-1} min^{-1}) and $t_{\max,N}$ is the time-to-max glucagon absorption constant. In (13), k_N is the glucagon elimination rate constant. The basal glucagon plasma concentration is given by N_b and the glucagon distribution volume by V_N. p is the rate constant of the glucagon action dynamics and S_N is the glucagon sensitivity.

D. Nonlinear state-space model

Let us conclude the section by collecting the equations described in the previous subsections into a nonlinear state-space model, which can be used for control-oriented simulations:

$$\begin{aligned}\dot{\boldsymbol{x}}(t) = \Big[&\dot{Q}_1(t)\ \dot{Q}_2(t)\ \dot{x}_1(t)\ \dot{x}_2(t)\ \dot{x}_3(t)\ \dot{S}_1(t)\ \dot{S}_2(t)\\ &\dot{I}(t)\ \dot{Z}_1(t)\ \dot{Z}_2(t)\ \dot{N}(t)\ \dot{Y}(t)\Big]^\top = \boldsymbol{f}(\boldsymbol{x}(t),\boldsymbol{u}(t))\end{aligned} \tag{15a}$$

$$\boldsymbol{y}(t) = G(t) = \boldsymbol{h}(\boldsymbol{x}(t),\boldsymbol{u}(t)) \tag{15b}$$

In Equation (15), $\dot{\boldsymbol{x}}(t)$ is the derivative of the state vector, consisting of the states described in Subsections II-A to II-C. The input vector is defined by insulin and glucagon infusion: $\boldsymbol{u}(t) = [u_I(t), u_N(t)]^\top$. The nonlinear vector function $\boldsymbol{f}(\boldsymbol{x}(t),\boldsymbol{u}(t))$ consists of the corresponding differential equations from Equations (1), (2) and (7)–(14), respectively. The output, $\boldsymbol{y}(t)$, is the BG concentration and therefore $\boldsymbol{h}(\boldsymbol{x}(t),\boldsymbol{u}(t))$ is defined by Equation (5).

III. Model predictive control design

The glucose intake through meals follows a relatively predictable pattern which motivates the use of MPC. In the following, with *linearized* MPC (LIN-MPC), we mean that a linearization of the nonlinear system dynamics is used to generate a prediction. Unfortunately, with a static linearization of the nonlinear dynamics, model accuracy (and therefore, closed-loop performance) is lost in practice. To mitigate that, the linearization used in each time step of the optimal control problem can be updated, based on the simulated trajectory of the previous iteration. This is the main principle of *linear time-varying* MPC (LTV-MPC) [23].

A. Linearized model predictive control

Let us consider a zero-order-hold discretization with sampling time $h = 15$ min as used in [12]:

$$\boldsymbol{x}_\Delta(k+1) = A\boldsymbol{x}_\Delta(k) + B\boldsymbol{u}_\Delta(k) + B_\mathrm{d}U_G(k) \tag{16a}$$

$$\boldsymbol{y}_\Delta(k) = C\boldsymbol{x}_\Delta(k) + D\boldsymbol{u}_\Delta(k) + D_\mathrm{d}U_G(k), \tag{16b}$$

where $\boldsymbol{x}_\Delta(k) = \boldsymbol{x}_\mathrm{L}(k) - \bar{\boldsymbol{x}}$, $\boldsymbol{u}_\Delta(k) = \boldsymbol{u}(k) - \bar{\boldsymbol{u}}$ and $\boldsymbol{y}_\Delta(k) = \boldsymbol{y}_\mathrm{L}(k) - \bar{\boldsymbol{y}}$ denote the deviations of linearized states $\boldsymbol{x}_\mathrm{L}$, inputs $\boldsymbol{u}$ and linearized outputs $\boldsymbol{y}_\mathrm{L}$ from the point around which the process of Equation (15) is linearized, respectively. The matrices B_d and D_d denote the influence of the gut absorption rate U_G (considered to be an exogenous disturbance input) on the states and output, respectively.

Next, we construct a cost function suited for glucoregulation with two requirements for safe BG control. First, a steady-state intravenous glucose level of 6 mmol L^{-1} is generally considered "optimal" [13]. Thus, we solve the steady-state problem for the continuous-time nonlinear dynamics of Section II with $G(t) = 6$ mmol L^{-1} to determine a state and input references, $\boldsymbol{x}_r$ and $\boldsymbol{u}_r$ (basal insulin and glucagon infusions). In turn, the cost function should penalize deviations from these references, so to keep the BG level close to $G(t) = 6$ mmol L^{-1}. Secondly, hypoglycemia should be avoided [24], hence it should be penalized strongly by the cost function, especially to avoid scenarios where hypoglycemia is preferred over hyperglycemia. To incorporate this idea into the objective function, we design an asymmetric term, such that hypoglycemic BG concentrations are penalized more heavily. Specifically, we add $\max\{0, G_r - G\}$ as a convex asymmetric term in the cost function, to penalize trajectories below $G_r = 6$ mmol L^{-1}. Overall, our proposed cost function reads as

$$\begin{aligned}J_N(i) = \ &\tfrac{1}{2}\sum_{k=i}^{i+N-1}\left(\|\boldsymbol{x}_\mathrm{L}(k+1|i) - \boldsymbol{x}_r\|_Q^2 + \|\boldsymbol{u}(k|i) - \boldsymbol{u}_r\|_R^2\right.\\ &\left. + c\,\max\{0, G_r - G(k|i)\}\right),\end{aligned} \tag{17}$$

where the index $(k|i)$ denotes the prediction of a certain variable (e.g. state variable) at time step k, given the value of the known variables (e.g. states and inputs) at time i ($k \geq i$). At each time step, LIN-MPC solves the following optimization problem to compute the control input:

$$\begin{cases}\min & J_N(i)\\ \text{s.t.} & \text{(16) holds, } \forall k \in \{i, i+1, \dots, i+N-1\}\\ & \boldsymbol{x}_\mathrm{min} \leq \boldsymbol{x}(k+1|i) \leq \boldsymbol{x}_\mathrm{max},\\ & \qquad\qquad \forall k \in \{i, \dots, i+N-1\}\\ & \boldsymbol{u}_\mathrm{min} \leq \boldsymbol{u}(k|i) \leq \boldsymbol{u}_\mathrm{max},\\ & \qquad\qquad \forall k \in \{i, \dots, i+N-1\}\end{cases} \tag{18}$$

where the minimum is taken over the control inputs $\boldsymbol{u}(i|i), \boldsymbol{u}(i+1|i), \cdots, \boldsymbol{u}(i+N-1|i)$. In Equation (18), i is the current discrete time, $\boldsymbol{x}_\mathrm{min}$ and $\boldsymbol{u}_\mathrm{min}$, $\boldsymbol{x}_\mathrm{max}$ and $\boldsymbol{u}_\mathrm{max}$ denote lower and upper bounds on the states and inputs. The measured current state $\boldsymbol{x}(i)$ is used as the initial condition for the current prediction. Let $\{\boldsymbol{u}^*(i|i), \boldsymbol{u}^*(i+1|i), \dots, \boldsymbol{u}^*(i+N-1|i)\}$ denote the optimal control input sequence that solves the optimization problem in (18). As usual in MPC, only the first input $\boldsymbol{u}^*(i|i)$ is applied to the dynamical system.

B. Linear time-varying model predictive control strategy

In this paper, we propose to use LTV-MPC for glucose regulation. Essentially, a sequence of linear process models is found at each time step by linearizing the dynamics (15) around the simulated trajectory and inputs obtained from the previous iteration [23]. This improves the accuracy of the process model used for control, thus resulting in better glucose disturbance rejection with respect to linearized MPC.

For the initial iteration, no prior knowledge on states or input is available, so at first the linearized MPC strategy is used. Solving the optimal control problem in (18) results in a sequence of optimal inputs $\{\boldsymbol{u}^*(0|0), \boldsymbol{u}^*(1|0), \dots, \boldsymbol{u}^*(N-1|0)\}$. While the first input is applied to the process, resulting in state $\boldsymbol{x}(1)$, all other inputs are supplied *in silico* to the dynamics (15), resulting in simulated states $\{\boldsymbol{x}(2|0), \boldsymbol{x}(3|0), \dots, \boldsymbol{x}(N+1|0)\}$. Let us define the *tail* of the trajectory at time 0 as:

$$\begin{cases}\{\boldsymbol{x}(1), \boldsymbol{x}(2|0), \dots, \boldsymbol{x}(N+1|0)\},\\ \{\boldsymbol{u}^*(1|0), \boldsymbol{u}^*(2|0), \dots, \boldsymbol{u}^*(N-1|0), \boldsymbol{u}(N|0)\}.\end{cases} \tag{19}$$

In each subsequent iteration i, the tail of the trajectory at time $i-1$ is used to obtain a time-varying linearization of the dynamics. Specifically, to obtain the linearized dynamics at time k during iteration i, the continuous-time state space model (15) is linearized analytically around the corresponding state-input pair $(\boldsymbol{x}(k|i-1), \boldsymbol{u}(k|i-1))$ from the tail of the trajectory at time $i-1$. To evaluate the matrices governing the linearization, we use the following partial derivatives:

$$A_{\text{cont}}(k|i-1) = \frac{\partial \boldsymbol{f}(\boldsymbol{x},\boldsymbol{u})}{\partial \boldsymbol{x}}(\boldsymbol{x}(k|i-1), \boldsymbol{u}(k|i-1)) \quad (20a)$$

$$B_{\text{cont}}(k|i-1) = \frac{\partial \boldsymbol{f}(\boldsymbol{x},\boldsymbol{u})}{\partial \boldsymbol{u}}(\boldsymbol{x}(k|i-1), \boldsymbol{u}(k|i-1)) \quad (20b)$$

$$B_{\text{d,cont}}(k|i-1) = \frac{\partial \boldsymbol{f}(\boldsymbol{x},\boldsymbol{u})}{\partial U_G}(\boldsymbol{x}(k|i-1), \boldsymbol{u}(k|i-1)) \quad (20c)$$

$$C(k|i-1) = \frac{\partial \boldsymbol{h}(\boldsymbol{x},\boldsymbol{u})}{\partial \boldsymbol{x}}(\boldsymbol{x}(k|i-1), \boldsymbol{u}(k|i-1)) \quad (20d)$$

$$D(k|i-1) = \frac{\partial \boldsymbol{h}(\boldsymbol{x},\boldsymbol{u})}{\partial \boldsymbol{u}}(\boldsymbol{x}(k|i-1), \boldsymbol{u}(k|i-1)) \quad (20e)$$

$$D_{\text{d}}(k|i-1) = \frac{\partial \boldsymbol{h}(\boldsymbol{x},\boldsymbol{u})}{\partial U_G}(\boldsymbol{x}(k|i-1), \boldsymbol{u}(k|i-1)) \quad (20f)$$

Then, we discretize this time-varying linearization via a zero-order hold with sampling time $h = 15$ min:

$$\begin{aligned}\boldsymbol{x}_\Delta(k+1|i) = {} & A(k|i-1)\boldsymbol{x}_\Delta(k|i) + B(k|i-1)\boldsymbol{u}_\Delta(k|i) \\ & + B_{\text{d}}(k|i-1)U_G(k)\end{aligned} \quad (21a)$$

$$\begin{aligned}\boldsymbol{y}_\Delta(k|i) = {} & C(k|i-1)\boldsymbol{x}_\Delta(k|i) + D(k|i-1)\boldsymbol{u}_\Delta(k|i) \\ & + D_{\text{d}}(k|i-1)U_G(k)\end{aligned} \quad (21b)$$

For the LTV-MPC problem, we design a cost function that is similar to that in (17), where the state predictions are replaced with their time-varying counterparts:

$$\begin{aligned}J_N(i) = \tfrac{1}{2} \sum_{k=i}^{i+N-1} & (\|\boldsymbol{x}_{\text{LTV}}(k+1|i) - \boldsymbol{x}_r\|_Q^2 + \|\boldsymbol{u}(k|i) - \boldsymbol{u}_r\|_R^2 \\ & + c\max\{0, G_r - G\}).\end{aligned} \quad (22)$$

The optimal control problem has then the same form as in (18), with the sole difference that the model dynamics now vary at each iteration and at each time step.

C. Controller tuning

Control guidelines for proper and safe intravenous glucose level regulation are established in [25]. First of all, the time spent in hyperglycemia should be minimized [26] and hypoglycemia should be avoided to ensure that patients do not fall into coma [24]. Secondly, a steady-state intravenous glucose level of 6 mmol L^{-1} is considered optimal, with glucose levels between 3.9 mmol L^{-1} and 7.8 mmol L^{-1} (normoglycemia) being considered safe [13]. Furthermore, the hyperglycemic peak, i.e. the maximum of the intravenous glucose level during hyperglycemia, should be small [26]. Lastly, minimal amounts of both insulin and glucagon should be applied. For insulin, this is done to avoid hypoglycemia as much as possible; instead, application of glucagon in high doses may result in nausea [20] and hence it should be avoided.

Tuning the MPC can be done through the weights Q, R and c, to be chosen in view of the mentioned three guidelines. Thus, based on *in silico* numerical experience, we have selected a state-weight $Q_{11} = 3 \cdot 10^4$ which acts only on the intravenous glucose mass state Q_1. In this way, the controller strongly penalizes hyperglycemia, which results in a very small hyperglycemia duration and a very small hyperglycemic peak. To avoid overly aggressive control actions, weights are placed on both the insulin and glucagon infusion. Importantly, we use off-diagonal input weights to discourage the controller from using insulin and glucagon simultaneously. The resulting input weighting matrix is then $R = 10^4 \cdot \left[\begin{smallmatrix} 8 & 2 \\ 2 & 100 \end{smallmatrix}\right]$.

Based on numerical experience, we have chosen the asymmetric cost weight $c = 5 \cdot 10^7$ such that plasma glucose concentrations below 6 mmol L^{-1} are significantly penalized. Finally, we choose state and input constraints such that all states and inputs are non-negative, as negative states or inputs are not physically possible. Furthermore, the maximum insulin infusion is chosen as 4 U h^{-1} and the maximum glucagon infusion is chosen as 15 μg kg^{-1} h^{-1}. In fact, we prefer not to constrain the states any further, as this could result in numerical feasibility and convergence problems.

IV. Numerical experiments

We simulate the system dynamics under the LIN-MPC and LTV-MPC strategies. The aim is to evaluate if the designed controller satisfies the performance requirements. Namely, hypoglycemia should be avoided, the hyperglycemic peak and duration should be minimal, a steady-state value of $G(t) = 6$ mmol L^{-1} should be attained quickly and minimal amounts of insulin and glucagon should be infused. As these requirements are inherently conflicting (e.g. not infusing insulin results in a higher hyperglycemic peak and duration), we perform some parameter tuning to assess if the proposed controller is able balance out the performance requirements properly. In particular, we tune the control horizon to $N = 12$.

A. Linear-time-varying vs linear-time-invariant MPC

We first consider the response of the LTV-MPC controller to a standardized meal disturbance of 80 g at $t = 0$ min, as shown in Fig. 1. The meal disturbance is rejected well by the LTV-MPC controller, with the disturbance response having a short hyperglycemia duration of around 2 hours (126 minutes) and a plasma glucose concentration peak of 14.48 mmol L^{-1}. At time $t = 45$ min, the LTV-MPC identifies that the optimal control action is to start administering glucagon, which allows for a more aggressive insulin infusion because it ensures no hypoglycemia occurs. The lowest glucose concentration value is 4.91 mmol L^{-1}, well within the highlighted region of normoglycemia. Fig. 1 also compares the response of the LTV-MPC controller to that of LIN-MPC with the same weights Q, R and c. Fig. 1 clearly shows that LTV-MPC results in a better response. The LIN-MPC response shows an undesirable hypoglycemic dip and duration (2.60 mmol L^{-1}, 207 min).

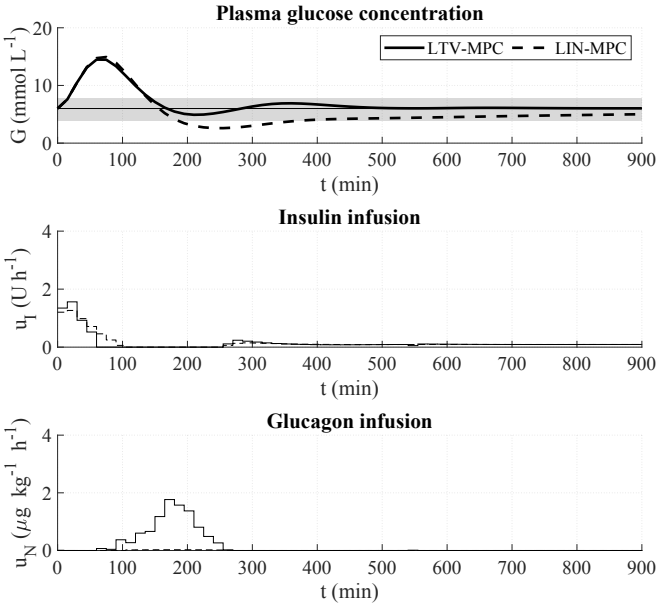

Fig. 1. Simulated closed-loop responses with linear time-varying (LTV-MPC) and linearized (LIN-MPC) model predictive controllers to a standardized meal disturbance of 80 g at $t = 0$ min. In the top sub-figure, normoglycemia is highlighted in grey and the target blood glucose concentration is denoted by a line at 6 mmol L^{-1}.

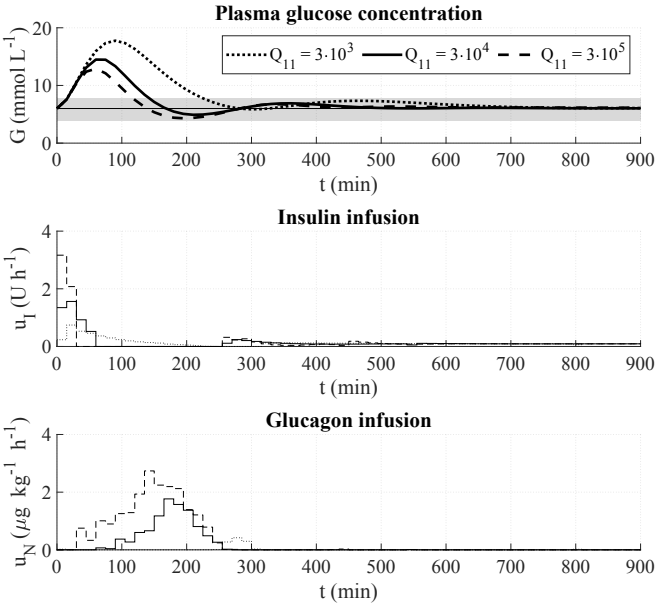

Fig. 2. Simulated closed-loop response with linear time-varying model predictive controller (LTV-MPC) to a standardized meal disturbance of 80 g at $t = 0$ min, for different primary state weights Q_{11}. In the top sub-figure, normoglycemia is highlighted in grey and the target blood glucose concentration is denoted by a line at 6 mmol L^{-1}.

B. Tuning the cost weight

Fig. 2 illustrates the influence of the weight matrix Q. For $Q_{11} = 3{\cdot}10^3$, we see that the hyperglycemic peak and duration (17.76 mmol L^{-1}, 208 min) are significantly larger than those for higher values of Q_{11}, as state deviations from the reference state are of less importance. This peak and duration do not satisfy the performance requirements. On the other hand, since input deviations from the reference input are penalized more strongly, the infused insulin and glucagon values are small. The contrary is true for $Q_{11} = 3 \cdot 10^5$, as state deviations are penalized more than input deviations. The result is a large initial insulin bolus (3.17 U h^{-1}) and a smaller hyperglycemic peak and duration (12.90 mmol L^{-1}, 102 min). However, the simulation for $Q_{11} = 3 \cdot 10^5$ also shows a dip below the target glucose value (4.30 mmol L^{-1}) and hypoglycemia is only avoided with a large glucagon infusion, which is against the performance requirements. For $Q_{11} = 3 \cdot 10^4$, which is the state weight we have chosen, the hyperglycemic peak and duration are only slightly larger than those for $Q_{11} = 3 \cdot 10^5$, while low glucose concentration values are avoided.

C. Bi-hormonal vs insulin only

Fig. 3 compares the proposed bi-hormonal LTV-MPC of Section III with a LTV-MPC that uses insulin as only control input. By constraining the glucagon input in the optimization problem to be zero, the model used for simulation is effectively the same as in [12] and as defined in Subsections II-A and II-B. Both simulations show approximately the same state trajectory initially. This can be expected, as both controllers can infuse insulin to mitigate the meal disturbance. However, the insulin-only controller reaches a hypoglycemic glucose concentration 3.52 mmol L^{-1}, where the bi-hormonal controller uses the glucagon input to prevent hypoglycemia. This implies that the bi-hormonal controller can be tuned more aggressively as opposed to the insulin-only controller and supports the use of glucagon in glucoregulatory control indeed.

D. Sensitivity to process parameters

Fig. 4 shows the simulation results of the LTV-MPC, where the process dynamics use the patient parameters in Table A. For patients 1 and 2, there is thus a mismatch between the parameters of the nonlinear process and the process simulated by the controller. These simulations show that accurate knowledge of the process parameters is important to properly regulate the plasma glucose concentration. In particular for the parameters of patient 1, the peak glucose plasma concentration grows to 17.31 mmol L^{-1} and the settling time increases to 310 min. For patient 2, the highest glucose concentration decreases to 13.58 mmol L^{-1}. Due to the mismatch in parameters the simulations for patient 1 and 2 both show a steady state error in the glucose concentration. This implies that they can be tuned more aggressively if the controller knows an accurate representation of the model parameters. Online parameter estimation, such as the approach presented in [12], can thus result in improved performance.

Fig. 5 shows the simulation results of the LTV-MPC for multiple meal disturbances, where the time-to-maximum carbohydrate absorption was varied in the process dynamics (but not in the controller). In the simulations, all disturbances are standardized meals, as described in Equation (6), of 80 gram

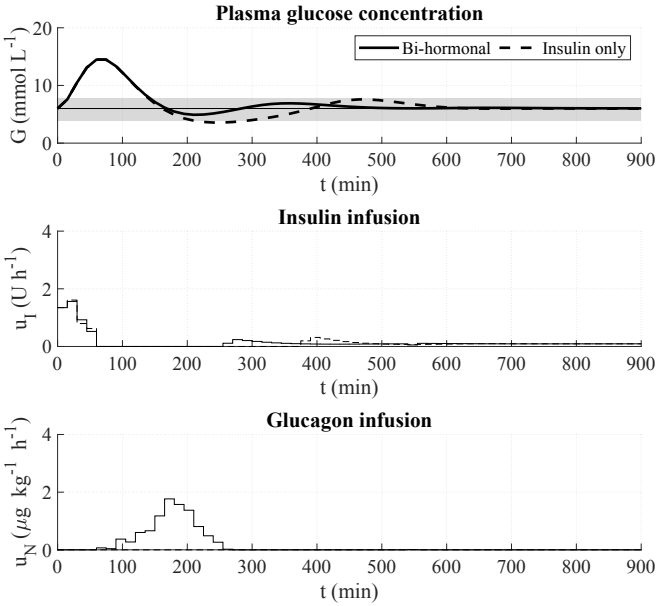

Fig. 3. Simulated closed-loop response with linear time-varying model predictive controller (LTV-MPC) to a standardized meal disturbance of 100 g at $t = 0$ min, with and without glucagon input. In the top sub-figure, normoglycemia is highlighted in grey and the target blood glucose concentration is denoted by a line at 6 mmol L^{-1}.

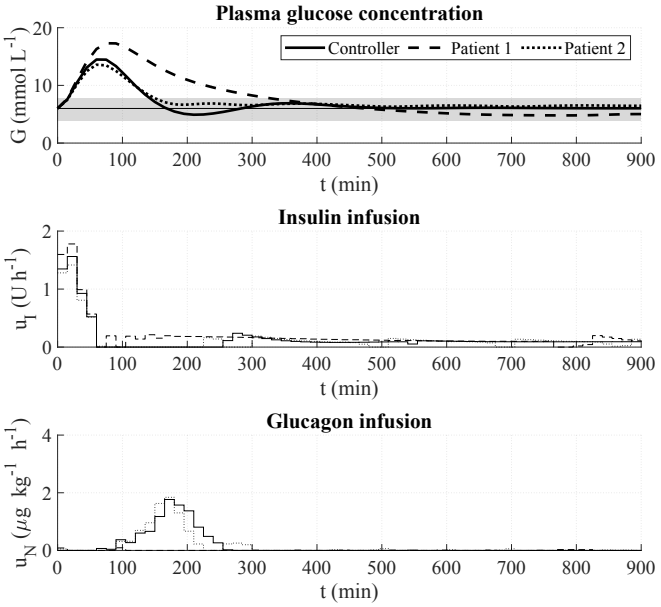

Fig. 4. Simulated closed-loop response with linear time-varying model predictive controller (LTV-MPC) to a standardized meal disturbance of 80 g at $t = 0$ min, where the process dynamics use the patient parameters in Table A. In the top sub-figure, normoglycemia is highlighted in grey and the target blood glucose concentration is denoted by a line at 6 mmol L^{-1}.

starting at $t = 0$ min. The time-to-maximum carbohydrate absorption for these disturbances is $t_{\max,G} \in \{28, 40, 52\}$ min.

For $t_{\max,G} = 28$ min, we find that the highest glucose concentration is 18.13 mmol L^{-1}, with a settling time of 120 min. For $t_{\max,G} = 52$ min, the highest glucose concentration is 12.12 mmol L^{-1}, with a settling time of 120 min. The reason for this is that the time-to-maximum carbohydrate absorption affects both the amplitude and the duration of the meal disturbance. If the time-to-maximum carbohydrate absorption increases, the amplitude of the meal disturbance grows, while the duration of the meal disturbance is reduced. As the controller does not have an accurate representation of $t_{\max,G}$, we also see these effects in the closed-loop response.

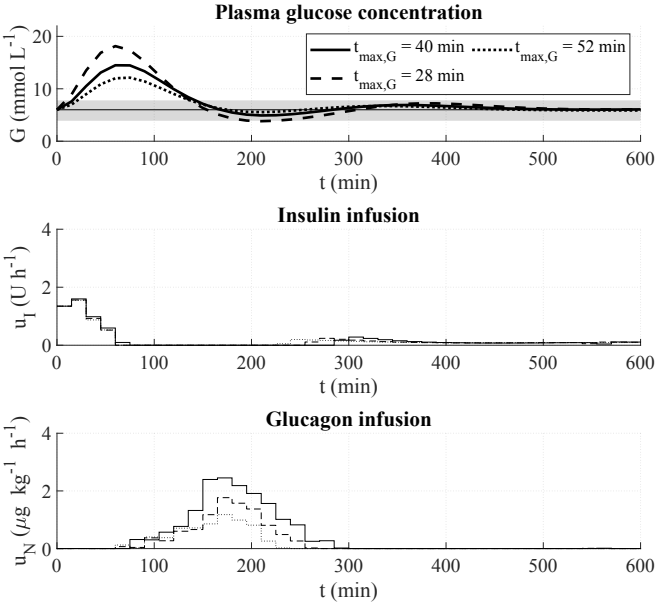

Fig. 5. Simulated closed-loop responses with linear time-varying model predictive controller (LTV-MPC) to a standardized meal disturbance of 80 g starting at $t = 0$ min, where the time-to-maximum carbohydrate absorption is varied in the process dynamics. In the top sub-figure, normoglycemia is highlighted in grey and the target blood glucose concentration is denoted by a line at 6 mmol L^{-1}.

V. Conclusion

Bi-hormonal linear-time-varying model predictive control is a promising method for regulating blood glucose concentration in patients with type 1 diabetes mellitus with much improved performance compared to standard model-based control. Future research should focus on the observability of the state variables and on the practical applicability of the method.

References

[1] P. Saeedi, I. Petersohn, P. Salpea, B. Malanda, S. Karuranga, N. Unwin, S. Colagiuri, L. Guariguata, A. A. Motala, K. Ogurtsova, J. E. Shaw, D. Bright, and R. Williams, "Global and regional diabetes prevalence estimates for 2019 and projections for 2030 and 2045: Results from the international diabetes federation diabetes atlas, 9th edition," *Diabetes Research and Clinical Practice*, vol. 157, p. 107843, Nov. 2019.

[2] W. H. Organization and I. D. Federation, "Definition and diagnosis of diabetes mellitus and intermediate hyperglycaemia : report of a who/idf consultation," p. p., 2006.

[3] P. E. Cryer, "The barrier of hypoglycemia in diabetes," *Diabetes*, vol. 57, no. 12, pp. 3169–3176, Nov. 2008.

[4] J. I. Moon, S. J. and C. Y. Park, "Current advances of artificial pancreas systems: A comprehensive review of the clinical evidence," *Diabetes and Metabolism Journal*, vol. 45, pp. 813–839, 2021.

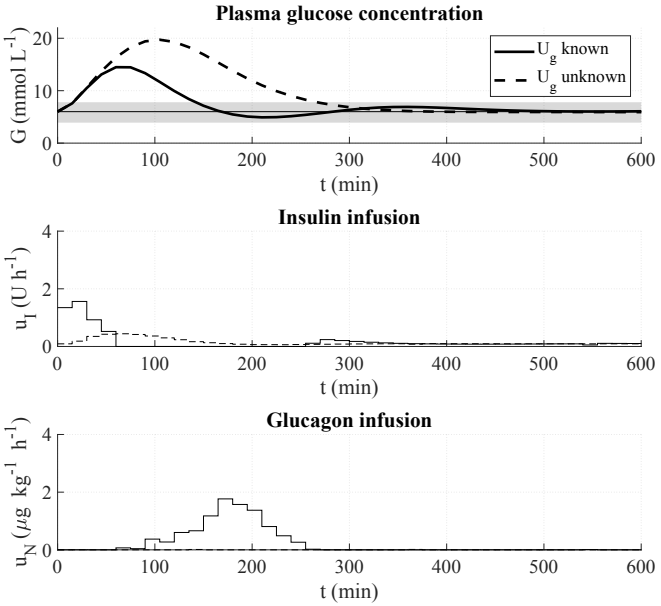

Fig. 6. Two simulated closed-loop responses with linear time-varying model predictive controller (LTV-MPC) to a standardized meal disturbance of 80 g at $t = 0$ min, where the disturbance is either completely known or unknown to the controller. In the top sub-figure, normoglycemia is highlighted in grey and the target blood glucose concentration is denoted by a line at 6 mmol L^{-1}.

[5] K. H. M. K. S. G. S. Benam, K. D. and A. L. Fougner, "Identifiable prediction animal model for the bi-hormonal intraperitoneal artificial pancreas," *Journal of Process Control*, vol. 121, pp. 13—-29, 2023.

[6] A. M. Albisser, B. S. Leibel, T. G. Ewart, Z. Davidovac, C. K. Botz, and W. Zingg, "An artificial endocrine pancreas," *Diabetes*, vol. 23, no. 5, pp. 389–396, 1974.

[7] E. Pfeiffer, C. Thum, and A. Clemens, "The artificial beta cell - a continuous control of blood sugar by external regulation of insulin infusion (glucose controlled insulin infusion system)," *Hormone and Metabolic Research*, vol. 6, no. 05, pp. 339–342, 1974.

[8] T. MohammadRidha, M. Ait-Ahmed, L. Chaillous, M. Krempf, I. Guilhem, J.-Y. Poirier, and C. H. Moog, "Model free iPID control for glycemia regulation of type-1 diabetes," *IEEE Transactions on Biomedical Engineering*, vol. 65, no. 1, pp. 199–206, Jan. 2018.

[9] F. Chee, T. Fernando, A. Savkin, and V. van Heeden, "Expert PID control system for blood glucose control in critically ill patients," *IEEE Transactions on Information Technology in Biomedicine*, vol. 7, no. 4, pp. 419–425, Dec. 2003.

[10] G. Marchetti, M. Barolo, L. Jovanovic, H. Zisser, and D. E. Seborg, "An improved PID switching control strategy for type 1 diabetes," *IEEE Transactions on Biomedical Engineering*, vol. 55, pp. 857–865, 2008.

[11] C. Man, M. Camilleri, and C. Cobelli, "A system model of oral glucose absorption: Validation on gold standard data," *IEEE Transactions on Biomedical Engineering*, vol. 53, no. 12, pp. 2472–2478, Dec. 2006.

[12] R. Hovorka, V. Canonico, L. J. Chassin, U. Haueter, M. Massi-Benedetti, M. O. Federici, T. R. Pieber, H. C. Schaller, L. Schaupp, T. Vering, and M. E. Wilinska, "Nonlinear model predictive control of glucose concentration in subjects with type 1 diabetes," *Physiological Measurement*, vol. 25, no. 4, pp. 905–920, Jul. 2004.

[13] R. Parker, F. Doyle, and N. Peppas, "The intravenous route to blood glucose control," *IEEE Engineering in Medicine and Biology Magazine*, vol. 20, no. 1, pp. 65–73, 2001.

[14] Z. Trajanoski and P. Wach, "Neural predictive controller for insulin delivery using the subcutaneous route," *IEEE Transactions on Biomedical Engineering*, vol. 45, no. 9, pp. 1122–1134, 1998.

[15] R. Parker, F. Doyle, and N. Peppas, "A model-based algorithm for blood glucose control in type i diabetic patients," *IEEE Transactions on Biomedical Engineering*, vol. 46, no. 2, pp. 148–157, 1999.

[16] L. Magni, D. M. Raimondo, L. Bossi, C. D. Man, G. D. Nicolao, B. Kovatchev, and C. Cobelli, "Model predictive control of type 1 diabetes: An in silico trial," *Journal of Diabetes Science and Technology*, vol. 1, no. 6, pp. 804–812, Nov. 2007.

[17] C. Lackinger, F. Reiterer, D. Moser, P. Schrangl, and L. del Re, "Chance-constrained model predictive control for blood glucose management in diabetes," in *IEEE Conference on Decision and Control*, Dec. 2017.

[18] S. Schaller, J. Lippert, L. Schaupp, T. R. Pieber, A. Schuppert, and T. Eissing, "Robust PBPK/PD-based model predictive control of blood glucose," *IEEE Transactions on Biomedical Engineering*, vol. 63, no. 7, pp. 1492–1504, Jul. 2016.

[19] P. Herrero, P. Georgiou, N. Oliver, M. Reddy, D. Johnston, and C. Toumazou, "A composite model of glucagon-glucose dynamics for in silico testing of bihormonal glucose controllers," *Journal of Diabetes Science and Technology*, vol. 7, no. 4, pp. 941–951, Jul. 2013.

[20] U. Hövelmann, B. V. Bysted, U. Mouritzen, F. Macchi, D. Lamers, B. Kronshage, D. V. Møller, and T. Heise, "Pharmacokinetic and pharmacodynamic characteristics of dasiglucagon, a novel soluble and stable glucagon analog," *Diabetes Care*, vol. 41, pp. 531–537, 2018.

[21] R. Hovorka, F. Shojaee-Moradie, P. V. Carroll, L. J. Chassin, I. J. Gowrie, N. C. Jackson, R. S. Tudor, A. M. Umpleby, and R. H. Jones, "Partitioning glucose distribution/transport, disposal, and endogenous production during IVGTT," *American Journal of Physiology-Endocrinology and Metabolism*, vol. 282, no. 5, pp. E992–E1007, 2002.

[22] R. N. Bergman, Y. Z. Ider, C. R. Bowden, and C. Cobelli, "Quantitative estimation of insulin sensitivity." *American Journal of Physiology-Endocrinology and Metabolism*, vol. 236, no. 6, p. E667, Jun. 1979.

[23] B. Kouvaritakis, M. Cannon, and J. A. Rossiter, "Non-linear model based predictive control," *International Journal of Control*, vol. 72, pp. 919–928, 1999.

[24] "Continuous glucose monitoring and intensive treatment of type 1 diabetes," *New England Journal of Medicine*, vol. 359, p. 1464, 2008.

[25] A. Ceriello and S. Colagiuri, "International diabetes federation guideline for management of postmeal glucose: a review of recommendations," *Diabetic Medicine*, vol. 25, no. 10, pp. 1151–1156, Oct. 2008.

[26] M. A. Atkinson, G. S. Eisenbarth, and A. W. Michels, "Type 1 diabetes," *Lancet*, vol. 383, no. 9911, pp. 69–82, Jan 2014.

APPENDIX A
MODEL PARAMETERS

parameter	unit	controller	patient 1*	patient 2*
V_G	L/kg	0.16	0.18	0.14
k_{12}	min^{-1}	0.0660	0.0343	0.0968
F_{01}	mmol/(kg min)	0.0097	0.0121	0.0119
EGP_0	mmol/(kg min)	0.0161	0.0148	0.0213
A_g	-	0.8	0.8	0.8
$t_{\max,G}$	min	40	40	40
$t_{\max,I}$	min	55	55	55
V_I	L kg^{-1}	0.12	0.12	0.12
k_e	min^{-1}	0.138	0.138	0.138
k_{a1}	min^{-1}	0.0060	0.0031	0.0088
k_{a2}	min^{-1}	0.0600	0.0752	0.0302
k_{a3}	min^{-1}	0.0300	0.0472	0.0118
$k_{b1} \cdot k_{a1}^{-1}$	L/(min mU)	$51.2{\cdot}10^{-4}$	$29.4{\cdot}10^{-4}$	$86.1{\cdot}10^{-4}$
$k_{b2} \cdot k_{a2}^{-1}$	L/(min mU)	$8.2{\cdot}10^{-4}$	$0.9{\cdot}10^{-4}$	$4.7{\cdot}10^{-4}$
$k_{b3} \cdot k_{a3}^{-1}$	L/mU	$520{\cdot}10^{-4}$	$401{\cdot}10^{-4}$	$720{\cdot}10^{-4}$
$t_{\max,N}$	min	15.76	32.46	20.59
k_N	min^{-1}	0.383	0.620	0.735
V_N	mL kg^{-1}	29.20	16.06	23.46
p	min^{-1}	0.164	0.016	0.074
$S_N \cdot 10^{-4}$	mL/pg min^{-1}	1.45	1.96	1.98
M_g	g/mol	180.16	180.16	180.16
BW	kg	68.5	68.5	68.5